Dielectric spectroscopy of liquid crystals in smectic, nematic, and isotropic phases confined in random porous media

G. P. Sinha and F. M. Aliev
Department of Physics and Materials Research Center, P.O. Box 23343, University of Puerto Rico, San Juan, PR 00931-3343, Puerto Rico
(Received 20 January 1998; revised manuscript received 27 March 1998)

The dielectric behavior of alkylcyanobiphenyls (5CB and 8CB) confined in porous matrices with randomly oriented, interconnected pores with two different mean pore sizes (1000 and 100 Å) has been investigated by means of broadband dielectric spectroscopy in the frequency range from 1 mHz to 1.5 GHz. The confinement has a strong influence on the dielectric properties of liquid crystals (LCs), which resulted in the appearance of a low frequency relaxation process ($f \leqslant 10$ kHz) not present in bulk and a second new process due to the presence of surface layer at solid pore wall-LC interface. Bulklike relaxation processes due to the rotation of molecules around the short axis and due to tumbling of molecules are also observed. All observed relaxation processes are of non-Debye type. Other observed differences between bulk and confined behavior are as follows: (a) the relaxation processes in confined LCs are not frozen even at temperatures about 20 degrees below the bulk crystallization temperature; (b) in the temperature range corresponding to the anisotropic phase in pores, the temperature dependence of the relaxation times (τ) of the process due to the rotation of molecules around the short axis is non-Arrhenius; (c) the retardation factor $g = \tau/\tau_{is}$ is $\simeq 1.5$, whereas the typical value of g in bulk nematic LCs is $\simeq 4$. At the nematic-isotropic phase transition in pores smooth and small changes in τ suggest that the "isotropic" phase of LCs in pores is not bulklike isotropic phase with complete disorder in molecular orientations, and some degree of orientational order still persists. [S1063-651X(98)05008-9]

PACS number(s): 61.30.−v, 77.22.Gm, 64.70.Md

I. INTRODUCTION

Studies of structure, phase, and glass transitions, as well as the dynamic behavior of complex fluids confined in porous media, have been very useful in exploring the fundamental physics of condensed matter. However, the results of these investigations are often puzzling and contradictory. The confinement of fluids can lead to such prominent changes in the physical properties that, even in the case of a one component isotropic fluid, a clear physical picture explaining these changes has not been achieved [1–11]. A variety of new properties and phenomena such as modification of phase transitions, orientational order, elastic properties, and director field, have been studied both experimentally and theoretically for liquid crystals (LCs) confined in random porous networks [12–25], as well as in cylindrical pores [26–34] (for review see also [35–39]).

Most of the recent investigations of confined LCs have not emphasized finite size and surface effects always present in porous media. Rather, attention has been focused on the effects of disorder on phase transitions and on the dynamics of fluctuations. One of the approaches used for the explanation of properties and behavior of confined LCs, as in the case of binary liquid mixtures (BLMs) confined in random porous matrices [40–46], is based on random-field-type models. Other approaches do not use this model at all. In the first study [15] of the nematic ordering of 8CB in sintered porous silica by the dynamic and static light scattering it was found that LC shows orientational glasslike dynamics near the nematic-isotropic phase transition. The main mechanism that determines the observed temporal fluctuation of the intensity of scattered light is the order parameter fluctuations. These fluctuations in the nematiclike state are very slow and glasslike. The equilibrium phase transition is smeared out by the randomness, and dynamically the system exhibits [15] the kind of self-similarity that is associated with the conventional random-field behavior. It was shown [15] that some features of the dynamic behavior of this system can be explained on the basis of the model in which porous medium imposes a random uniaxial field on the LC.

In another investigation [19] of the dynamic properties of 8CB confined in an aerogel host by dynamic light scattering the observed dynamic behavior was different from that in sintered porous silica [15]. Nevertheless according to Ref. [19] the spin glass interpretation given by these authors and the random field interpretation given in [15] are consistent if the geometrical differences between two matrices are taken into account. The orientational dynamics of 5CB confined in nanometer-length-scale porous silica glass was investigated by time-resolved transient grating optical Kerr effect [47] in the temperature range corresponding to the bulk deep isotropic phase. A nonexponential relaxation and a distribution of relaxation times were observed. The pore size dependence of relaxation times was explained from the point of view of the Landau model applied to independent pore segments. However, this model and the distribution of the pore sizes do not describe the nonexponential form of the decay.

Structural aspects of the influence of confinement on 8CB in aerogel matrix were studied [16] using light scattering and calorimetry. Some features of nematic ordering in the aerogel porous matrix were qualitatively explained in terms of the random-field Ising model with an asymmetric distribution of random fields. Later it was mentioned [20] that the same random-field argument [16] is qualitatively consistent with the results of NMR investigations of LCs in aerogel.

The modification of weakly first-order nematic-isotropic and second order nematic to smectic-*A* transitions were ob-

served [48] in high-resolution ac calorimetric study of 8CB in silica aerogels. It was found [48] that the explanation of the changes in peak height and peak position (on the temperature scale) of the excess heat capacity relative to the bulk values can be explained on the basis of theoretically proposed [49] quenched random field effects, while these changes cannot be represented as finite-size effects.

The absence of a nematic-isotropic phase transition and gradual increase of the local orientational order was observed [17] in NMR and calorimetric studies on 5CB in Vycor porous glass with average pore size about 75 Å. These results were satisfactorily described by taking into account the ordering effects of surface interactions and the disordering effects due to surface induced deformations. The Landau-type theory was used, and a random-field theory Hamiltonian was not needed. There was no need to involve consideration based on the random-field model to explain the results of magnetically induced birefringence measurements [18] for 5CB in Vycor-like porous glass having 100 Å pore size. The sigmoidal temperature dependence of the Cotton-Mouton coefficient is consistent with the changes in the direction and possibly the magnitude of nonzero tensor order parameter, even above the bulk nematic-isotropic phase transition temperature. In the most recent study [25] of optical power of a chiral LC confined in random porous matrix the difference between bulk and confined behavior was attributed to a combination of surface and finite-size effects without involving the random-field-based models. Although great success in the understanding of physical properties of LCs confined in porous media with different size and shape of pores and different structure of porous matrix was achieved, little work has been done to characterize the influence of confinement on the different aspects of dynamical behavior of confined LC. Dielectric spectroscopy can be applied to investigate multiple aspects of the influence of confinement on dynamic properties of LCs. This method contributes significantly to the overall characterization of porous materials [50] in general, and investigations of condensed matter confined to porous media in particular. Applications of dielectric spectroscopy to glass-forming liquids [51–55] and confined LCs [14,56–60] revealed new information on the changes in the molecular mobility, the broadening of the distribution of relaxation times, as well as changes in the phase and the glass transition temperatures. Dielectric spectroscopy applied to bulk nematic and smectic-*A* LCs studies dynamical processes of molecular origin. In the bulk phases of these LCs there are no dielectric relaxation processes associated with the order parameter since there is no polar ordering and therefore dynamics of order parameter is not involved. Since randomness first of all influences the ordering, dielectric properties of confined LCs should be less sensitive, or not sensitive at all to the presence of random fields imposed by random porous structure. Instead the influence of the interface, in our case the solid pore wall-liquid crystal interface, as well as size effects due to confinement become very important. The confinement can break the symmetry of the bulk phase, and change viscosity, which can lead to a modification of the dynamics of molecular motion. In the case of LCs composed of polar molecules, the presence of the interface and spatial restriction may induce a polar ordered layer at the interface and give rise to polarization effects, which can also be due to a gradient of the order parameter and inhomogeneity of orientation. Clearly, the bent nature of the pore may induce these effects in porous matrices.

In this paper we report on a comprehensive study of the dielectric properties of pentylcyanobiphenyl (5CB) and octylcyanobiphenyl (8CB) confined to porous glass matrices with randomly oriented, interconnected pores with mean pore sizes of 1000 and 100 Å. The confinement in matrices of 1000 Å pore size is interesting in particular. It is natural to assume that in the case of large pore size (say, greater than the correlation length) the behavior of confined material should be close to that in bulk. However, the investigations of BLM confined in 1000 Å pores showed significant differences [43] in its dynamical behavior from that in the bulk. In the case of LCs, the distances at which the influence of the solid-LC interface is essential, are extended up to thousands of angstroms [61], and it is important to compare the results for two very different pore sizes. Broadband dielectric spectroscopy in the frequency range 10^{-3} Hz–1.5×10^{9} Hz was applied to investigate the influence of the confinement on the dynamical behavior of the LCs in the isotropic, nematic, and smectic phases.

The dielectric properties of the bulk 4-*n*-alkyl-4′-cyanobiphenyls have been studied extensively [62–69] and have been quite clearly understood. In the nematic phases of 5CB and 8CB, in a geometry in which the electric field **E** is parallel to the director **n**, i.e., $\mathbf{E}\|\mathbf{n}$, [62–65] the real (ϵ') and imaginary (ϵ'') parts of the dielectric permittivity have a dispersion region with a characteristic frequency at about 5 MHz. This dispersion is due to the restricted rotation of the molecules about their short axis and is of Debye type, i.e., it has a single relaxation time. The temperature dependence of the corresponding relaxation times (τ) obeys the empirical Arrhenius equation. The activation energies are approximately 58.5 kJ/mol for 5CB [62] and 66.2 kJ/mol for 8CB in the nematic phase [68]. In the smectic phase of 8CB, for the same orientation of the electric field, the relaxation time slightly increases. The corresponding activation energy is 44.2 kJ/mol [68]. For the geometry in which the electric field **E** is perpendicular to the director **n**, $\mathbf{E}\perp\mathbf{n}$, dielectric investigations were performed using the conventional frequency domain spectroscopy, for both 5CB and 8CB [63–65] and time domain spectroscopy for 8CB [66,67]. In this geometry the most prominent relaxation process with characteristic frequency about 70 MHz was observed. In a recent dielectric investigation of 5CB in cylindrical porous membrane this process has been attributed to the tumbling of the molecules [56]. The dielectric properties of the isotropic phase of these LCs are also well known. In this phase, the characteristic relaxation frequencies corresponding to the molecular rotation of 5CB and 8CB are around 20 MHz. The respective activation energies are 27.8 kJ/mol [69] and 28.8 kJ/mol [66].

We show that the confinement has a strong influence on the dielectric properties of LCs. The paper is organized as follows. In Sec. II we describe our samples and the experimental setup. The information on phase transition temperatures of the investigated LCs in pores is also given in this Section. In Sec. III we present the broadband dielectric spectra in the frequency range 10^{-3} Hz–1.5 GHz for 8CB confined in 1000 Å and 100 Å pores. The main goal of this

section is to provide general information on all possible dispersion regions present in confined alkylcianobiphenyls. We show that the observed dielectric spectra, along with two bulklike processes, have new relaxation processes absent in bulk LCs. In Sec. IV we present the dielectric spectra at different temperatures for processes corresponding to bulklike relaxation, and discuss the size effect. We show that the bulklike processes have some features typical for glass forming organic liquids. Section V is devoted to a discussion of temperature dependence of relaxation times of bulklike processes.

II. EXPERIMENT

A. Samples

We used porous silica glasses with randomly oriented and interconnected pores as matrices. The mean sizes of the pores were 100 Å and 1000 Å. The corresponding volume fractions of the pores were 27% and 40%, respectively. These matrices were solid plates in square shape with flat and parallel surfaces. The dimensions of the glass plate were 25 mm$\times$25 mm$\times$1 mm. The porous silica glasses have negligible electrical conductivity, and their dielectric permittivity is practically independent of frequency and temperature. We impregnated these porous glasses with liquid crystals 5CB and 8CB at temperatures corresponding to isotropic phase. The bulk 5CB has a nematic phase in the temperature range of 22.5–35 °C. 8CB has a smectic phase in the temperature range of 21.1–33.5 °C in addition to the nematic range of 33.5–40.8 °C. Since the pores are distributed randomly in the matrices, therefore independently of alignment of LCs on pore walls, there are molecules oriented both parallel as well as perpendicular to the direction of probing electric field. This means that the dielectric behavior typical for two geometries $\mathbf{E}\|\mathbf{n}$ and $\mathbf{E}\perp\mathbf{n}$ should be detected in the same experiment.

B. Measurement

Measurements of the real (ϵ') and the imaginary (ϵ'') parts of the complex dielectric permittivity in the frequency range 10^{-3} Hz to 1.5 GHz were performed using two sets of devices. In the range from 10^{-3} Hz to 3 MHz we used the Schlumberger Technologies 1260 Impedance/Gain-Phase Analyzer in combination with Novocontrol Broad Band Dielectric Converter and an active sample cell (BDC-S). The BDC-S, which includes the active sample cell, the sample holder, the sample capacitor, high precision reference capacitors, and active electronics, optimizes the overall performance and reduces the typical noise in the measurements, particularly at low frequencies. The sample was mounted between two gold plated parallel plates and placed in the shielded cell. For measurements in the frequency range 1 MHz—1.5 GHz we used Hewlett-Packard 4291A rf Impedance Analyzer in combination with a high temperature test head and a calibrated Hewlett-Packard 16453A Dielectric Material Test Fixture. In this frequency range measurements were performed at 200 different frequencies with averaging done over 300 times at each frequency. The accuracy of the temperature stabilization was better than 0.1 °C.

For the quantitative analysis of the dielectric spectra the Havriliak-Negami function [70] has been used. For the case

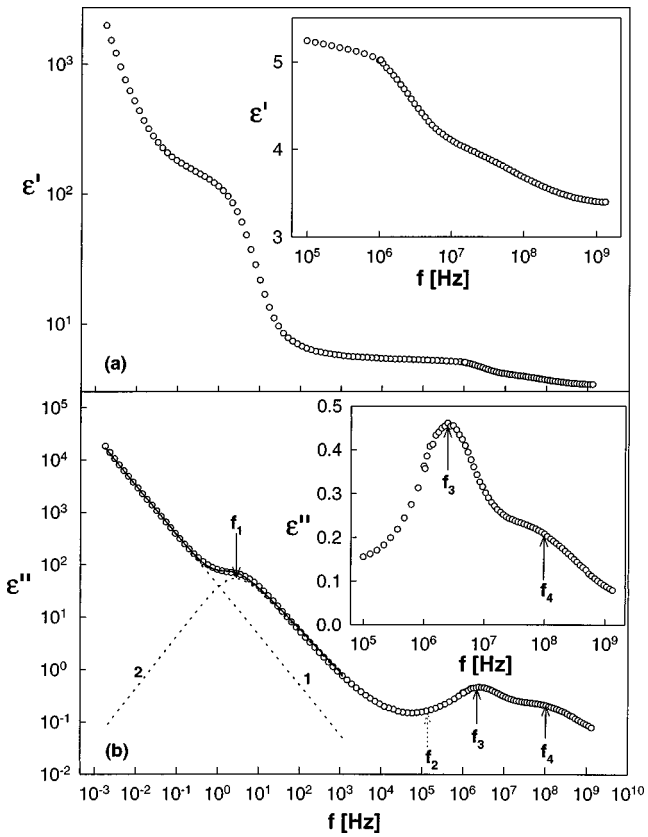

FIG. 1. Dielectric spectrum of 8CB in 1000 Å random pores for $T=295$ K: (a) real part, (b) imaginary part. Open circles: experiment, solid line: fitting; 1: contribution from conductivity, 2: relaxation process. The insets show the details of the high frequency processes. The arrows indicate the characteristic frequencies of different observed relaxation processes.

of more than one relaxation process, taking into account the contribution of the dc conductivity to the imaginary part of dielectric permittivity, the Havriliak-Negami function is given by

$$\epsilon^* = \epsilon_\infty + \sum_j \frac{\Delta\epsilon_j}{[1+(i2\pi f\tau_j)^{1-\alpha_j}]^{\beta_j}} - i\frac{\sigma}{2\pi\epsilon_0 f^n}, \qquad (1)$$

where ϵ_∞ is the high-frequency limit of the permittivity, $\Delta\epsilon_j$ the dielectric strength, τ_j the mean relaxation time, and j the number of the relaxation process. The exponents α_j and β_j describe the symmetric and asymmetric distribution of relaxation times. The term $i\sigma/2\pi\epsilon_0 f^n$ accounts for the contribution of conductivity σ, with n as fitting parameter. In the case of pure Ohmic conductivity $n=1$. The decrease of n, i.e., $n<1$, could be observed, as a rule, if in addition to the contribution to ϵ'' from conductivity, there is an influence of electrode polarization.

III. BROADBAND DIELECTRIC SPECTRA OF CONFINED LIQUID CRYSTAL

The dielectric behavior of confined LCs that we investigated is very different from its behavior in bulk. It is illustrated in Figs. 1 and 2. These two figures represent the typical example of the broadband dielectric spectra that we

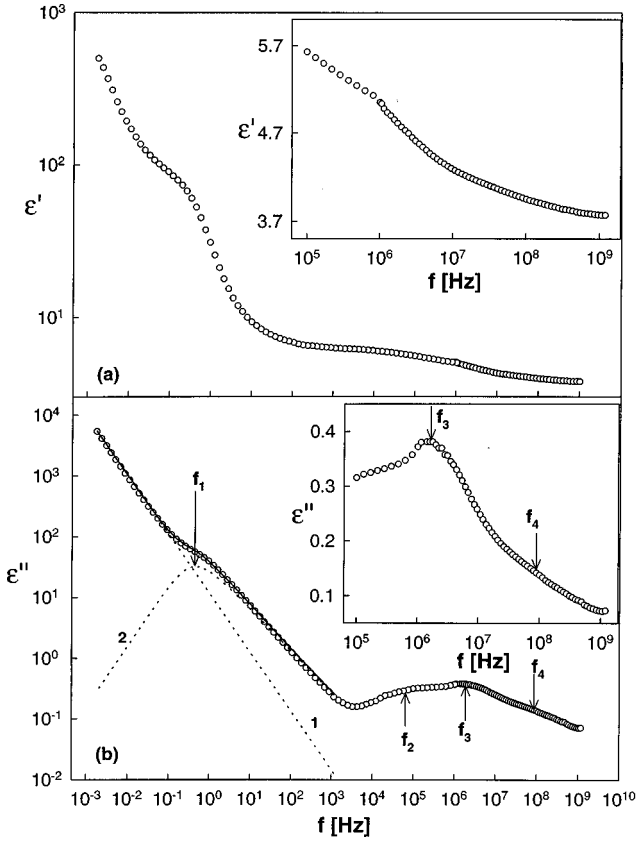

FIG. 2. Dielectric spectrum of 8CB in 100 Å random pores for $T=295$ K: (a) real part, (b) imaginary part. Open circles: experiment; solid line: fitting; 1: contribution from conductivity, 2: relaxation process. The insets show the details of the high frequency processes. The arrows indicate the characteristic frequencies of different observed relaxation processes.

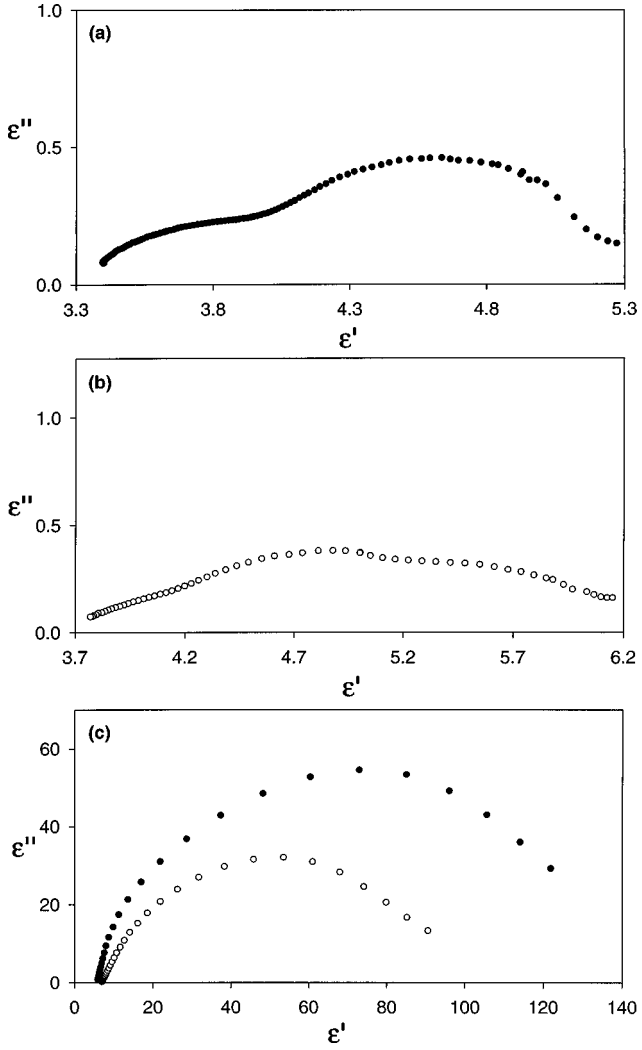

FIG. 3. Cole-Cole plots for $T=295$ K: (a) and (b) high frequency and (c) low frequency data. Open circles: 8CB in 1000 Å; closed circles: 100 Å pores.

observe for confined LCs. It is clear from Fig. 1 that for 8CB confined in 1000 Å, at least four dispersion regions could be obviously identified: a very slow process (10^{-3}–1 Hz), a second wide process (1–10^4 Hz), a very clear process in MHz frequency range and the last one in the frequency range $f>30$ MHz which is also visible without detailed analysis. The last two processes are clearly separated as can be seen in insets (a) and (b) in Fig. 1 as well as from the corresponding Cole-Cole plot in Fig. 3(a). The influence of the pore size on the dielectric behavior is illustrated in Fig. 2 in which the dielectric spectrum for 8CB confined in 100 Å is presented. In addition to the processes observed in 1000 Å pores, there is a new process below the MHz frequency range in 100 Å pores immediately after the first two low frequency dispersions. This process can also be identified from the corresponding Cole-Cole plot in Fig. 3(b). Detailed data analysis shows that for both 5CB and 8CB in 1000 Å pores this process is barely seen but is also present in the pores. The highest frequency relaxation process is less noticeable in 100 Å pores than in 1000 Å, however it is distinct from the Cole-Cole plot in Fig. 3 (b).

From Figs. 1 and 2 it is obvious that the dielectric spectra for 5CB and 8CB are complicated. For simplicity we analyze the data for frequencies $f<1$ kHz separately. Application of formula (1) for data analysis shows that the strong frequency dependence of ϵ'' for $f<0.1$ Hz is due to Ohmic conductivity and the contribution from the electrode polarization is negligibly small. The contribution from conductivity is perfectly described by the dotted lines (1) in Figs. 1 and 2 with the parameters presented in Table I. After the subtraction of the contribution from conductivity described by the second term in formula (1), the frequency dependencies of ϵ'' are represented by the dotted lines (2) in Figs. 1 and 2. These dependencies have relaxation origin and are quantitatively described by the Havriliak-Negami formula. The parameters α, β, Δ, ϵ, and τ describing these processes observed for 8CB in 1000 Å and 100 Å pores are presented in Table I. We suggest that this low frequency process is the relaxation of

TABLE I. Parameters of the lowest frequency relaxation processes for confined 8CB at $T=295$ K.

$\sigma(10^{-9}\ \Omega^{-1}\ \mathrm{m}^{-1})$	n	$\Delta\epsilon$	$\tau\ (10^{-1}\ \mathrm{s})$	α	β
	8CB in 1000 Å pores				
2.0	0.95	120.7	0.71	0	0.7
	8CB in 100 Å pores				
0.66	0.97	76.6	4.6	0	0.8

the interfacial polarization arising at the pore wall-liquid crystal interface. The structure of the thin surface layer of LC on the solid surface, in our case pore wall, could be very different from the structure of the liquid crystal in bulk. For example, at the interface a layer with surface induced polar ordering may exist. In general, there might be two main reasons for the appearance of the layer with polar ordering: either absorption of ions at the LC–pore-wall interface or orientation of permanent dipoles due to polar interactions of molecular dipoles with solid surface.

Ion absorption in two component heterogeneous media gives rise to dispersion of dielectric permittivity, which develops according to the following scenario: for a mixture of two or more components the accumulation of charges at the interfaces between phases gives rise to a polarization that contributes to the relaxation if at least one component has nonzero electric conductivity. This phenomenon is known as the Maxwell-Wagner (MW) effect [71]. The relaxation time of the process due to the MW effect, taking into account that the conductivity of empty porous matrix is negligibly small compared to the conductivity of LCs, is given by

$$\tau_{\mathrm{MW}}=2\pi\epsilon_0\frac{2\epsilon_m+\epsilon+\omega(\epsilon_m-\epsilon)}{\sigma(1-\omega)}, \qquad (2)$$

where ϵ_m is the dielectric permittivity of the matrix material, ϵ the dielectric permittivity of the second component, in our case LCs and ω is the volume fraction of pores.

It is difficult to attribute the observed low frequency relaxation process to the MW relaxation. One can estimate the MW relaxation time using formula (2), $\epsilon_m=3.95$ and measured conductivities (Table I). The dielectric permittivity of the second component can vary in the following limits from $\epsilon_{\parallel}\approx 13$ to $\epsilon_{\perp}\approx 5.5$. We obtain the relaxation times (0.70–0.52) s for 1000 Å pores and (2.1–1.49) s for 100 Å pores. These calculated relaxation times are ten times slower than those determined by the experiment. If we take into account the high dielectric strength observed in the experiments, then a greater dielectric permittivity of LC should be used. In that case, the discrepancy between the experimental values of τ and the estimated τ_{MW} will increase by as much as a factor of 100. Additionally the low frequency process is not described by the Debye relaxation function as it should be for the MW relaxation and there is a spectrum of relaxation times. Most likely, there exists an interfacial polarization due to the formation of a surface layer on the pore wall with polar ordering. In this case a new cooperative and slow process may arise. The relaxation time of this process should be related to effective viscosity of LC, which can be greater in small pores than in large pores (since the volume fraction of the surface layer is greater in 100 Å pores). Even though the above analysis suggests a relaxation mechanism due to orientation of permanent dipoles at pore wall-liquid crystal interface rather than one due to the MW mechanism, it should be noted that the above analysis is very qualitative and all values are just estimates.

There is another new relaxation process in pores that does not exist in bulk LCs. The characteristic frequency of this process is identified as f_2 in Figs. 1 and 2. This relaxation is due to the rotation of molecules, located in the surface layer formed at pore walls. This process is slower than the process due to rotation of molecules in bulk because the viscosity in surface layers is greater than the bulk viscosity.

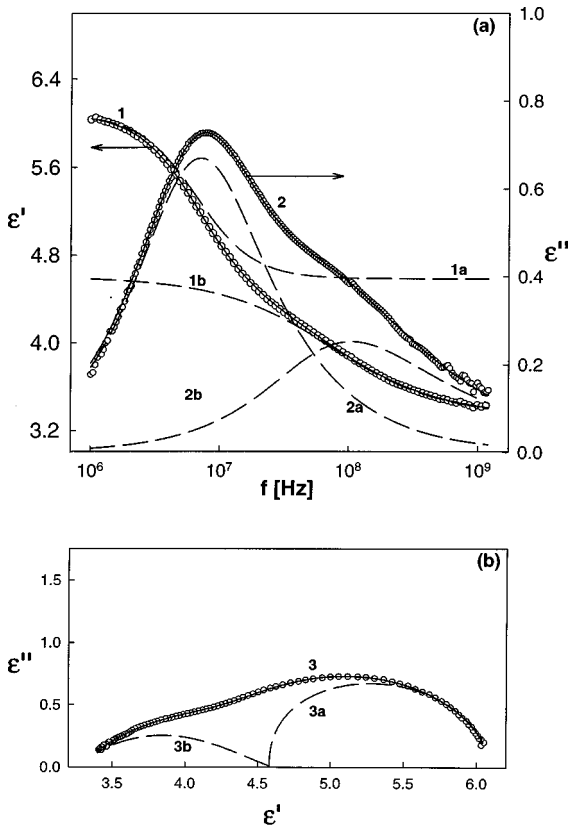

FIG. 4. (a) Dielectric spectrum and (b) Cole-Cole plot of 5CB in 1000 Å random pores for $T=303$ K. Open circles: experiment; solid lines: fitting. Dashed lines represent the separation of two processes.

The last two processes in the MHz and 100 MHz frequency range observed for both matrices are ''bulklike.'' The first one is due to the rotation of molecules about its short axis and the second one is due to the tumbling of the molecules about their molecular short axis. These two processes in pores, although having the same mechanism as in bulk, are strongly modified by confinement as we show below.

We found that all the observed relaxation processes are not frozen even at 20° below bulk crystallization temperature.

IV. BULKLIKE RELAXATION IN CONFINED 5CB AND 8CB IN ANISOTROPIC PHASES

We believe that the relaxation process with $\tau\sim 10^{-8}$ s for 5CB and 8CB in both porous matrices has the same origin as in bulk and corresponds to the rotation of the molecules, which do not belong to the surface layer, around the short axis. However, confinement has a strong effect on this process. A process with a distribution of relaxation times replaces the Debye-type relaxation process with a single relaxation time observed in bulk [62,68]. Figures 4, 5, and 6, show the frequency dependence of the real and imaginary parts of the dielectric permittivity of the bulklike processes for confined LCs. The solid lines in each of them represent

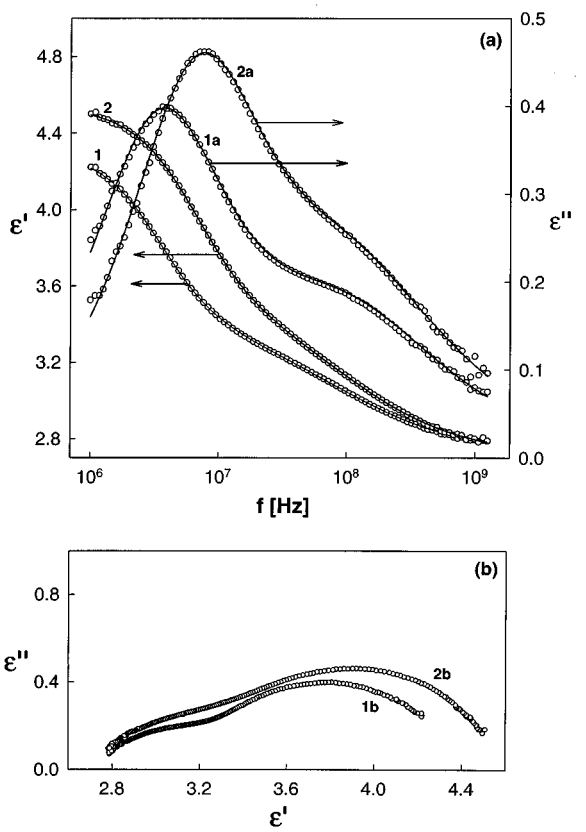

FIG. 5. (a) Dielectric spectra and (b) Cole-Cole plot of 8CB in 1000 Å for $T=300$ K (1, $1a$, and $1b$) and for $T=310$ K (2, $2a$, and $2b$). Open symbols: experiment; solid lines: fitting.

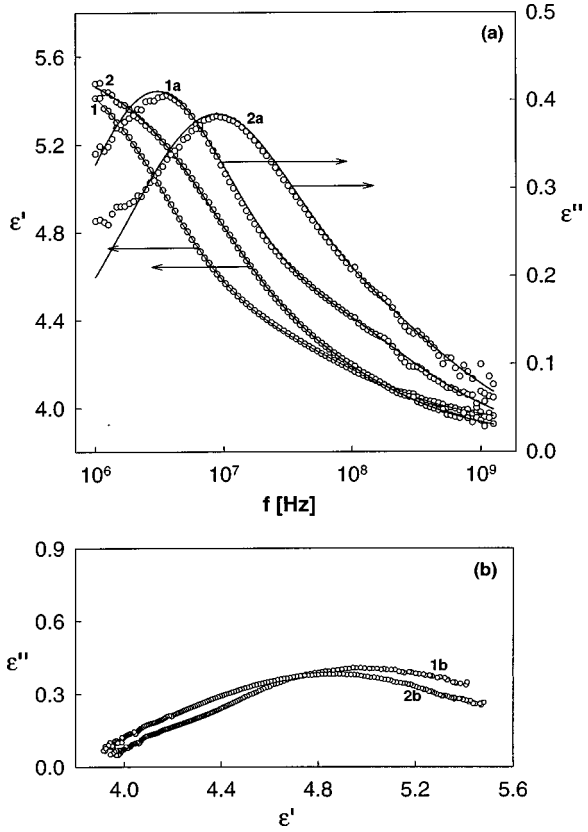

FIG. 6. (a) Dielectric spectra and (b) Cole-Cole plot of 8CB in 100 Å for $T=300$ K (1, $1a$, and $1b$) and for $T=310$ K (2, $2a$, and $2b$). Open symbols: experiment; solid lines: fitting.

the result of fitting by formula (1). Figure 4(a) shows the dielectric spectrum of 5CB in 1000 Å random pores at $T=303.1$ K and Fig. 4(b) is the corresponding Cole-Cole plot. Figures 5 and 6 represent the dielectric spectra and the corresponding Cole-Cole plots for 8CB in 1000 Å and 100 Å random pores, each measured at two different temperatures: 300 and 310 K. The comparison between data presented in Figs. 5 and 6 illustrates the pore size effect. The fitting parameters τ_1, α_1, β_1, τ_2, α_2, and β_2 describing the bulklike relaxation processes are presented in Table II.

A relaxation process at frequencies $f>50$ MHz has been observed in bulk alkylcyanobiphenyls for an orientation of the electric field perpendicular to the director [63–67]. One of the suggested explanations of the origin of this high frequency relaxation was given in terms of tumbling motion of molecules [60]. In random pores, there are always molecules oriented perpendicular to the electric field regardless of the molecular alignment inside pores. Therefore we assume that the process observed in the frequency range $f>50$ MHz has the same origin as was found earlier for bulk alkylcyanobiphenyls [63–67]. The presence of the process due to tumbling of molecules is obvious in our experiments without deep analysis, where as the existence of the high frequency relaxation in bulk alkylcyanobiphenyls was concluded on the basis of fitting procedure [63–65]. In 100 Å random pores, the amplitude of the last process was smaller than in 1000 Å pores. It should be mentioned that the Debye relaxation function does not describe bulklike relaxation processes in pores. Instead the dielectric function describing confined LCs is similar to that for glass forming systems. This is more clearly seen in the time domain representation. Figure 7 shows the experimental data for 8CB in 1000 and 100 Å pores obtained by the frequency domain measurements converted to the time domain. These data are described by the decay function that is a superposition of two stretched exponential functions:

$$1-\Psi(t)=ae^{-(t/\tau_1)^{\beta_1}}+(1-a)e^{-(t/\tau_2)^{\beta_2}}. \tag{3}$$

The transformation to the time domain is done by using the step answer function

$$1-\Psi(t)=\int_0^\infty G(\tau)\exp\left(-\frac{t}{\tau}\right)d\tau, \tag{4}$$

TABLE II. Parameters of bulklike relaxation processes for confined 5CB and 8CB.

T (K)	τ_1 (10^{-8} s)	α_1	β_1	τ_2 (10^{-9} s)	α_2	β_2
5CB in 1000 Å pores						
303.1	2.61	0	0.83	2.54	0.1	0.6
8CB in 1000 Å pores						
300.0	4.63	0.08	1	1.81	0.28	0.88
310.0	2.35	0.08	1	1.75	0.22	0.77
8CB in 100 Å pores						
300.0	5.56	0.25	1	1.91	0.19	0.72
310.0	1.95	0.30	1	0.80	0.23	0.88

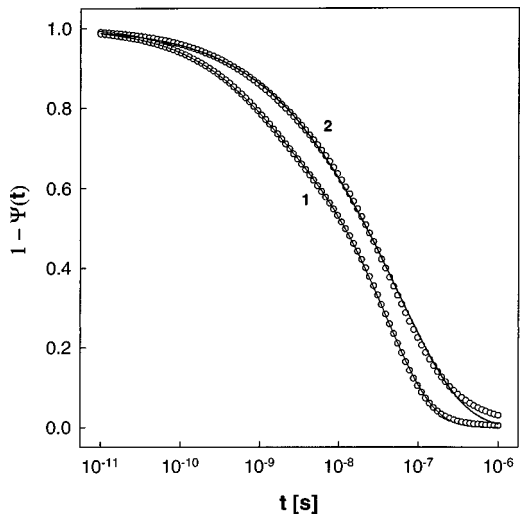

FIG. 7. Decay function for 8CB confined in 1000 Å (curve 1) and 100 Å (curve 2) pores at $T=300$ K. Open symbols: experiment; solid lines: fitting.

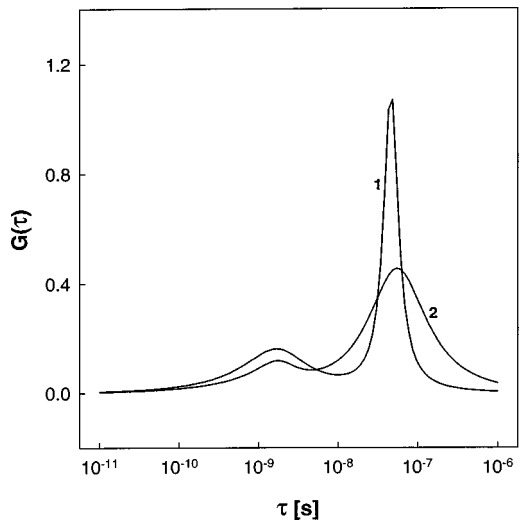

FIG. 8. Distribution of relaxation times for 8CB confined in 1000 Å (curve 1) and 100 Å (curve 2) pores.

where the relaxation time distribution function $G(\tau)$ for a superposition of j Havriliak-Negami terms is calculated by

$$G(\tau)=\frac{\sum_{i=1}^{j}\Delta\epsilon_i g_i(\tau)}{\sum_{i=1}^{j}\Delta\epsilon_i}. \tag{5}$$

The relaxation time distribution function for a single Havriliak-Negami term with parameters $\alpha_i,\beta_i,\tau_{0i},\Delta\epsilon_i$, is obtained as

$$g_i(\tau)=\frac{(\tau/\tau_{0i})^{\beta_i\alpha_i}\sin(\beta_i\Theta_i)}{\pi\tau[(\tau/\tau_{0i})^{2\alpha_i}+2(\tau/\tau_{0i})^{\alpha_i}\cos(\pi\alpha_i)+1]^{\beta_i/2}}, \tag{6}$$

where

$$\Theta_i=\arctan\left(\frac{\sin(\pi\alpha_i)}{\tau/\tau_{0i}+\cos(\pi\alpha_i)}\right), \tag{7}$$

and $0\leqslant\Theta\leqslant\pi$.

The solid lines in the figure correspond to the fitting function (3) with fitting parameters presented in Table III. The parameters a, τ_1, and $\overline{\beta}_1$ correspond to the process due to rotation of the molecules around their short axis and the parameters $(1-a)$, τ_2, and $\overline{\beta}_2$ take into account contribution from the high frequency molecular tumbling process. The amplitude of the process due to the rotation of molecules around the short axis is greater in narrow pores. Both of the processes represented in Fig. 7 are slower in 100 Å than in 1000 Å pores as observed for the low frequency relaxation process. The origin of the retardation of all the processes in narrow pores is the same. This is because the molecules farthest from the pore wall in narrow pores are at a distance less than 50 Å, whereas in large pores this distance could be as long as 500 Å. Therefore the influence of the interface on the dynamical behavior of molecules in narrow pores should be greater. Thus the retardation in the molecular motion in narrow pores is mainly due to interfacial effect. It is surprising that the dynamical processes due to molecular motion in pores have some features typical for glasslike dynamical behavior, although bulk LCs do not have glassy properties either in anisotropic or in isotropic phases. This modification of dynamical behavior in non-glass-forming liquids might be observed not only in pores but also in thin layers at the solid-liquid interface. The effect of pore size on the dynamical behavior of confined LCs could also be seen from the comparison of relaxation time distribution functions $G(\tau)$ presented in Fig. 8. This figure represents the result of the application of formula (5) for curve (1) of both Fig. 5 and Fig. 6. The spectrum of relaxation times is wider for 100 Å than for 1000 Å pores.

TABLE III. Autocorrelation function parameters of bulklike relaxation processes for confined 8CB at $T=300$ K.

a	τ_1 (10^{-8} s)	$\overline{\beta}_1$	τ_2 (10^{-9} s)	$\overline{\beta}_2$
	8CB in 1000 Å pores			
0.77	3.82	0.71	0.78	0.68
	8CB in 100 Å pores			
0.92	5.6	0.54	1.91	0.61

There are marked changes in the temperature dependence of the relaxation times compared to the bulk behavior. These changes and the influence of the pore size on the relaxation times are discussed in the next section.

V. TEMPERATURE DEPENDENCE OF RELAXATION TIMES OF BULKLIKE PROCESSES

The temperature dependence of the relaxation times corresponding to the rotation of molecules around the short axis for confined 5CB and 8CB are presented in Figs. 9 and 10. The observed dependencies are very different from the behavior typical for bulk LC. These differences provide us with the information on the influence of confinement on isotropic to nematic and nematic to smectic-A phase transitions. In Figs. 9 and 10, $\ln\tau$ in general is not a linear function of $1/T$ in the temperature range corresponding to the anisotropic

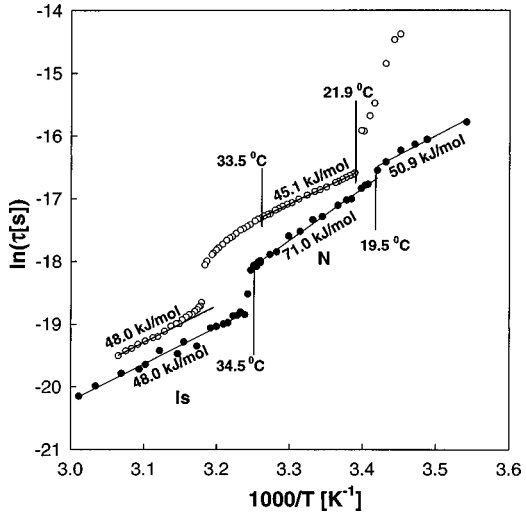

FIG. 9. Temperature dependence of relaxation times of the process due to the rotation of molecules around short axis. Closed circles: 5CB; open circles: 8CB in 1000 Å pores.

phases of confined 5CB and 8CB. The strongest deviations from the Arrhenius behavior are observed for LCs confined in 100 Å pores.

Data for 8CB in random pores show the influence of confinement on the nematic to smectic-*A* phase transition. In the temperature range corresponding to the liquid crystalline phases in pores, there are no abrupt changes in the relaxation times as for the bulk smectic-*A* to nematic phase transition. Instead, the relaxation times smoothly increase while the temperature varies from values corresponding to the nematic phase to that of the smectic-*A* phase. On the other hand the slope of the $\ln\tau$ versus $1/T$ (Figs. 9 and 10) slightly decreases in the temperature range corresponding to the smectic-*A* phase as for bulk LCs having nematic and smectic-*A* phases. We note two facts: the decrease in the slope of $\ln\tau$ versus $1/T$ and the smooth temperature dependence of the relaxation time. These lead to the conclusion that the smectic phase is still present in pores, however, the

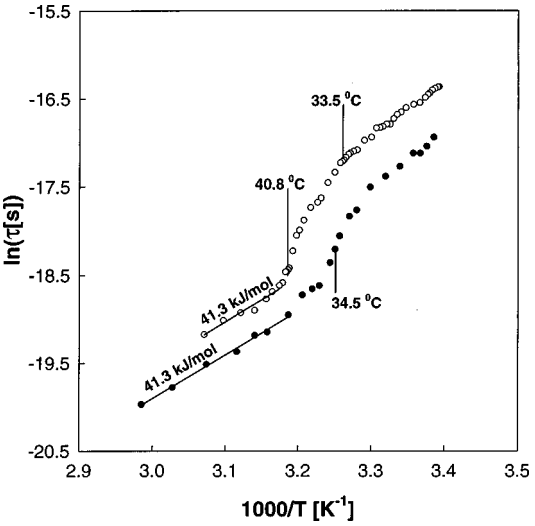

FIG. 10. Temperature dependence of relaxation times of the process due to the rotation of molecules around short axis. Closed circles: 5CB; open circles: 8CB in 100 Å pores.

smectic-*A* to nematic phase transition is considerably broadened. This observation is in agreement with the conclusions about the influence of random porous confinement on the smectic-*A* to nematic transition made on the basis of NMR and calorimetry investigations of confined 8CB [23,24]. For 8CB in 1000 Å pores the significant increase of relaxation times is observed at $T<21.9$ °C. This increase in the relaxation times could be related to the strong changes in viscosity due to supercooling of LC in pores much below the crystallization temperature.

The data for 5CB in 1000 Å pores are less complicated (note that bulk 5CB does not have a smectic phase). The behavior of 5CB confined in these pores is closer to that in bulk, and the deviations from the Arrhenius-type behavior are prominent in the vicinity of nematic-isotropic phase transition temperature. If we consider the temperature regions $34.5\ °\text{C}<T<20\ °\text{C}$ (ΔT_1) and $19.5\ °\text{C}<T<9\ °\text{C}$ (ΔT_2) separately, then we notice that the temperature dependence of τ in each of these regions is rather well approximated by the Arrhenius formula $\tau=\tau_0\exp(U/RT)$, where U is the activation energy and R is universal gas constant. The activation energies determined by fitting are $U_1=71$ kJ/mol and $U_2=50.9$ kJ/mol in the temperature ranges ΔT_1 and ΔT_2, respectively. The first activation energy U_1 is greater than the activation energy of bulk nematic phase ($U_b=58.5$ kJ/mol). We attribute the temperature range ΔT_1 to the nematic phase of 5CB in 1000 Å pores. The activation energy of the nematic phase in pores is greater than that in bulk because the pore wall imposes additional potential due to pore-wall–molecule interaction. This potential is determined by U_1-U_b. The corresponding magnitude of the potential energy of the molecule–pore-wall interaction per molecule is 2×10^{-20} J. Taking into account that the number of molecules per unit area is $(2-3)\times10^{18}$ m^{-2} we estimate the surface potential of molecule-wall interaction $U_{\text{surf}}\sim0.05$ J/m^2.

The activation energy U_2 is smaller than U_1 and U_b. The value of U_2 is very close to the value of activation energy of relaxation due to the rotation of molecules around short axis for 8CB in the same pores in the temperature range $21.9\ °\text{C}<T<33.5\ °\text{C}$, which corresponds to the smectic phase. This fact suggests that for 5CB in 1000 Å pores crystallization is replaced by short-range smectic type layering at the pore wall.

The activation energies of the relaxation process due to the rotation of molecules around the short axis in the isotropic phase of both 5CB and 8CB in 1000 Å pores is 48 kJ/mol. The relaxation times for 8CB are greater than for 5CB, as seen in Figs. 9 and 10, because 8CB is more viscous than 5CB. We also observe that the changes in relaxation times at the nematic-isotropic phase transition in pores for both LCs are not as sharp as in bulk, and the relaxation times in pores at the transition do not change as much as in bulk. The retardation factor $g=\tau/\tau_{is}$ at nematic-isotropic phase transition temperature for both of the investigated LCs in pores is $\simeq1.5$, where as the corresponding typical value of g for bulk nematic LCs is $\simeq4$. Relatively smooth and small changes in τ at phase transition in pores suggest that the ''isotropic'' phase of LCs in pores is not bulklike with complete disorder in molecular orientations, and some orientational order still persists.

The highest frequency process (due to molecular tumbling) was more visible in 1000 Å pores than in 100 Å pores as can be seen from Figs. 5 and 6. In bulk LCs this relaxation is observable only in the anisotropic phase in which the director is well defined, and this process vanishes in the isotropic (disordered) phase. The pore size dependence of the dielectric strength of the process due to the tumbling motion suggests that in anisotropic phases LCs in 100 Å pores macroscopically are less ordered than in 1000 Å pores. The influence of the disorder imposed by the random porous structure (geometrical disorder) affects the physical properties and phenomena that are mainly determined by the order at macroscopic scales.

We obtained that the relaxation times of the process due to tumbling of molecules for LCs confined in porous matrices are also temperature dependent [72]. This dependence can be approximated by the Arrhenius formula. For 5CB the activation energies are 28.8 and 23 kJ/mol in 100 and 1000 Å pores, respectively. For 8CB the activation energies are 33.6 and 25.9 kJ/mol in 100 and 1000 Å pores, respectively. The activation energies are greater in small pores because the role of the influence of the pore-wall–molecule interaction on reorientational dynamics is more important for pores of smaller size.

VI. CONCLUSION

The spatial confinement has a strong influence on the dielectric properties of LCs in isotropic, nematic, and smectic-*A* phases. The relaxation processes were not completely frozen even at temperatures at least 20 °C below the bulk crystallization temperature. Slow relaxation process that does not exist in the bulk phase and the process due to the presence of surface layer at the solid pore-wall–liquid crystal interface, in which the dynamics of molecular motion is different from that in the bulk, were observed. Modified bulklike relaxation processes due to the rotation of molecules around the short axis and due to the tumbling of molecules are also observed in confined geometry. The relaxation times of the tumbling process were found to be temperature dependent. All observed relaxation processes are non-Debye-type processes. Even for the bulklike processes, data analysis in the time domain representation shows that the decay function is stretch exponential, whereas it is single exponential for bulk LCs. This reveals the existence of a spectrum of relaxation times for each process with the width being broader for smaller pore size. The main differences in the dynamical behavior of confined LCs from that in the bulk, observed in dielectric spectroscopy experiments, are due to finite-size effects and the existence of the LC–pore-wall interface. Random structure of porous media has secondary importance.

ACKNOWLEDGMENTS

We thank Dr. F. Kremer, Dr. R. Richert, Dr. R. Stannarius, and Dr. J. Thoen for useful conversations. This work was supported by U.S. Air Force Grant No. F49620-95-1-0520, and NSF Grant No. OSR-9452893.

[1] *Molecular Dynamics in Restricted Geometries*, edited by J. Klafter and J. M. Drake (Wiley, New York, 1989).
[2] *Dynamics in Small Confining Systems*, edited by J. M. Drake, J. Klafter, R. Kopelman, and D. D. Awschalom, MRS Symposia Proceedings No. 290 (Materials Research Society, Pittsburgh, PA, 1993).
[3] *Dynamics in Small Confining Systems II*, edited by J. M. Drake, J. Klafter, R. Kopelman, and S. M. Troian, MRS Symposia Proceedings No. 363 (Materials Research Society, Pittsburgh, PA, 1995).
[4] *Dynamics in Small Confining Systems III*, edited by J. M. Drake, J. Klafter, and R. Kopelman, MRS Symposia Proceedings No. 464 (Materials Research Society, Pittsburgh, PA, 1997).
[5] J. Warnock and D. D. Awschalom, Phys. Rev. B **34**, 475 (1986).
[6] D. D. Awschalom and J. Warnock, Phys. Rev. B **35**, 6779 (1987).
[7] C. L. Jackson and G. B. McKenna, J. Chem. Phys. **93**, 9002 (1990).
[8] J.-P. Korb, S. Xu, and J. Jonas, J. Chem. Phys. **98**, 2411 (1993).
[9] J.-P. Korb, L. Malier, S. Xu, and J. Jonas, Phys. Rev. Lett. **77**, 2312 (1996).
[10] P. Pissis, D. Daoukaki-Diamanti, L. Apekis, and C. Christodoulides, J. Phys.: Condens. Matter **6**, L325 (1994).
[11] R. Richert, Phys. Rev. B **54**, 1 (1996).
[12] D. Armitage and F. P. Price, Chem. Phys. Lett. **44**, 305 (1976).
[13] D. Armitage and F. P. Price, Mol. Cryst. Liq. Cryst. **44**, 33 (1978).
[14] F. M. Aliev and M. N. Breganov, Sov. Phys. JETP **68**, 70 (1989).
[15] X.-L. Wu, W. I. Goldburg, M. X. Liu, and J. Z. Xue, Phys. Rev. Lett. **69**, 470 (1992).
[16] T. Bellini, N. A. Clark, C. D. Muzny, L. Wu, C. W. Garland, D. W. Schaefer, and B. J. Oliver, Phys. Rev. Lett. **69**, 788 (1992).
[17] G. S. Iannacchione, G. P. Crawford, S. Zumer, J. W. Doane, and D. Finotello, Phys. Rev. Lett. **71**, 2595 (1993).
[18] S. Tripathi, C. Rosenblatt, and F. M. Aliev, Phys. Rev. Lett. **72**, 2725 (1994).
[19] T. Bellini, N. A. Clark, and D. W. Schaefer, Phys. Rev. Lett. **74**, 2740 (1995).
[20] A. Zidansek, S. Kralj, G. Lahajnar, and R. Blinc, Phys. Rev. E **51**, 3332 (1995).
[21] Z. Zhang and A. Chakrabarti, Phys. Rev. E **52**, 4991 (1995).
[22] F. M. Aliev and V. V. Nadtotchi in *Disordered Materials and Interfaces*, edited by H. Z. Cummins, D. J. Durian, D. L. Johnson, and H. E. Stanley, MRS Symposia Proceedings No. 407 (Materials Research Society, Pittsburgh, PA, 1996), p. 125.
[23] S. Qian, G. S. Iannacchione, D. Finotello, Phys. Rev. E **53**, R4291 (1996).
[24] G. S. Iannacchione, S. Qian, D. Finotello, and F. M. Aliev, Phys. Rev. E **56**, 554 (1997).

[25] D. Kang, C. Rosenblatt, and F. Aliev, Phys. Rev. Lett. **79**, 4826 (1997).
[26] M. Kuzma and M. M. Labes, Mol. Cryst. Liq. Cryst. **100**, 103 (1983).
[27] G. P. Crawford, D. K. Yang, S. Zumer, D. Finotello, and J. W. Doane, Phys. Rev. Lett. **66**, 723 (1991).
[28] G. P. Crawford, D. W. Allender, and J. W. Doane, Phys. Rev. A **45**, 8693 (1992).
[29] M. Dadmun and M. Muthukumar, J. Chem. Phys. **98**, 4850 (1993).
[30] G. P. Crawford, R. Ondris-Crawford, S. Zumer, and J. W. Doane, Phys. Rev. Lett. **70**, 1838 (1993).
[31] R. J. Ondris-Crawford, G. P. Crawford, J. W. Doane, and S. Zumer, Phys. Rev. E **48**, 1998 (1993).
[32] N. Vrbancic, M. Vilfan, R. Blinc, J. Dolinsek, G. P. Crawford, and J. W. Doane, J. Chem. Phys. **98**, 3540 (1993).
[33] G. S. Iannacchione and D. Finotello, Phys. Rev. E **50**, 4780 (1994).
[34] K. A. Crandall, C. Rosenblatt, and F. M. Aliev, Phys. Rev. E **53**, 636 (1996).
[35] F. M. Aliev, in *Access in Nanoporous Materials*, edited by T.J. Pinnavaia and M.F. Thorpe (Plenum Press, New York, 1995), p. 335.
[36] D. Finotello and G. Iannacchione, Int. J. Mod. Phys. B **9**, 109 (1995).
[37] G. P. Crawford and S. Zumer, Int. J. Mod. Phys. B **9**, 331 (1995).
[38] P. S. Drzaic, *Liquid Crystal Dispersions* (World Scientific, Singapore, 1995).
[39] *Liquid Crystals in Complex Geometries Formed by Polymer and Porous Networks*, edited by G. P. Crawford and S. Zumer (Taylor & Francis, London, 1996).
[40] S. B. Dierker and P. Wiltzius, Phys. Rev. Lett. **58**, 1865 (1987).
[41] M. C. Goh, W. I. Goldburg, and C. M. Knobler, Phys. Rev. Lett. **58**, 1008 (1987).
[42] B. J. Frisken and D. S. Cannell, Phys. Rev. Lett. **69**, 632 (1992).
[43] F. M. Aliev, W. I. Goldburg, and X.-l. Wu, Phys. Rev. E **47**, R3834 (1993).
[44] W. I. Goldburg, F. Aliev, and X.-l. Wu, Physica A **213**, 61 (1995).
[45] M. Y. Lin, S. K. Sinha, J. M. Drake, X.-l. Wu, P. Thiyagarajan, and H. B. Stanley, Phys. Rev. Lett. **72**, 2207 (1994).
[46] S. Lacelle, L. Tremblay, Y. Bussiere, F. Cau, and C. G. Fry, Phys. Rev. Lett. **74**, 5228 (1995).
[47] G. Schwalb and F. W. Deeg, Phys. Rev. Lett. **74**, 1383 (1995).
[48] L. Wu, Z. Zhou, C. W. Garland, T. Bellini, and D. W. Schaefer, Phys. Rev. E **51**, 2157 (1995).
[49] A. Martian, M. Cieplak, T. Bellini, and J. R. Banavar, Phys. Rev. Lett. **72**, 4113 (1994).
[50] R. Hilfer, Phys. Rev. B **44**, 60 (1991).
[51] J. Schüller, Yu. B. Mel'nichenko, R. Richert, and E. W. Fischer, Phys. Rev. Lett. **73**, 2224 (1994).
[52] J. Schüller, R. Richert, and E. W. Fischer, Phys. Rev. B **52**, 15 232 (1995).
[53] Yu. B. Mel'nichenko, J. Schüller, R. Richert, B. Ewen, and C.-K. Loong, J. Chem. Phys. **103**, 2016 (1995).
[54] M. Arndt and F. Kremer, in *Dynamics in Small Confining Systems II*, edited by J. M. Drake, J. Klafter, R. Kopelman, and S. M. Troian, Materials Research Society Symposia Proceeding No. 363 (Materials Research Society, Pittsburgh, PA, 1995), p. 259.
[55] M. Arndt, R. Stannarius, W. Gorbatschow, and F. Kremer, Phys. Rev. E **54**, 5377 (1996).
[56] S. A. Rozanski, R. Stannarius, H. Groothues, and F. Kremer, Liq. Cryst. **20**, 59 (1996).
[57] F. M. Aliev and G. P. Sinha, in *Electrically based Microstructural Characterization*, edited by R.A. Gerhardt, S. R. Taylor, and E.J. Garboczi, MRS Symposia Proceedings No. 411 (Materials Research Society, Pittsburgh, PA, 1996), p. 413.
[58] Ch. Cramer, Th. Cramer, M. Arndt, F. Kremer, L. Naji, and R. Stannarius, Mol. Cryst. Liq. Cryst. Sci. Technol., Sect. A **304**, 209 (1997).
[59] G. P. Sinha and F. M. Aliev, Mol. Cryst. Liq. Cryst. Sci. Technol., Sect. A **304**, 309 (1997).
[60] Ch. Cramer, Th. Cramer, F. Kremer, and R. Stannarius, J. Chem. Phys. **106**, 3730 (1997).
[61] B. Jerome, Rep. Prog. Phys. **54**, 391 (1991).
[62] P. G. Cummins, D. A. Dunmur, and D. A. Laidler, Mol. Cryst. Liq. Cryst. Sci. Technol., Sect. A **30**, 109 (1975).
[63] J. M. Wacrenier, C. Druon, and D. Lippens, Mol. Phys. **43**, 97 (1981).
[64] C. Druon and J. M. Wacrenier, J. Phys. (France) **38**, 47 (1977).
[65] D. Lippens, J. P. Parneix, and A. Chapoton, J. Phys. (France) **38**, 1465 (1977).
[66] T. K. Bose, R. Chahine, M. Merabet, and J. Thoen, J. Phys. (France) **45**, 1329 (1984).
[67] T. K. Bose, B. Campbell, S. Yagihara, and J. Thoen, Phys. Rev. A **36**, 5767 (1987).
[68] A. Buka and A. H. Price, Mol. Cryst. Liq. Cryst. Sci. Technol., Sect. A **116**, 187 (1985).
[69] H.-G. Kreul, S. Urban, and A. Würflinger, Phys. Rev. A **45**, 8624 (1992).
[70] S. Havriliak and S. Negami, Polymer **8**, 101 (1967).
[71] B. K. P. Scaife, *Principles of Dielectrics* (Clarendon Press, Oxford, 1989).
[72] Compare this result with the observed temperature independence of the relaxation time of the process due to the tumbling motion reported in [68].